Acta Derm Venereol 2008; 88: 547–554

INVESTIGATIVE REPORT

Microscopic Distribution of Protoporphyrin (PpIX) Fluorescence in Superficial Basal Cell Carcinoma During Light-fractionated Aminolaevulinic Acid Photodynamic Therapy

Ellen R. M. DE HAAS[1], Henriette S. DE BRUIJN[2], Henricus J. C. M. STERENBORG[2], H. A. Martino NEUMANN[1] and Dominic J. ROBINSON[1,2]

[1]*Department of Dermatology, and* [2]*Centre of Optical Diagnostics and Therapy, Department of Radiation Oncology, Erasmus MC Rotterdam, The Netherlands*

Light fractionation in aminolaevulinic acid photodynamic therapy (PDT) of superficial basal cell carcinoma has been shown to enhance the therapeutic efficacy significantly. We have shown previously that this increase in efficacy is not simply due to an increase in the amount of protoporphyrin utilized during therapy. The present study investigated the spatial distribution of protoporphyrin in 32 superficial basal cell carcinomas undergoing light-fractionated PDT. Superficial fluorescence imaging performed during therapy was compared with the microscopic analysis of protoporphyrin fluorescence in biopsies acquired immediately before the second of two light fractions. The microscopic distribution of fluorescence was also compared with tumour sections immunohistochemically stained for Ki-67. Large variations in superficial and microscopic protoporphyrin fluorescence were found in both control and treated lesions. Despite these variations there was a reasonable correlation between the two techniques ($R^2 = 0.86$). The mean fluorescence intensity in control biopsies was greater than in illuminated lesions before the second light fraction, but there was no significant difference in the variation within and between regions of interest in each of these sets of lesions. There was no clear trend in depth of protoporphyrin reappearance during the dark interval between light fractions. The general distribution of cells stained positive for Ki-67 followed the protoporphyrin fluorescence that was associated with islands of basal cell carcinoma. In conclusion, this study confirms that the mean relative re-synthesis of protoporphyrin after PDT is consistent with that found previously in pre-clinical models. There are large variations in fluorescence within superficial basal cell carcinoma that include regions of tumour cells that do not synthesize protoporphyrin. ***Key words: ALA-PDT; basal cell carcinoma; PpIX; fluorescence kinetics; Ki57.***

(Accepted April 7, 2008.)

Acta Derm Venereol 2008; 88: 547–554.

Dominic J. Robinson, Center for Optical Diagnostics and Therapy, Department of Radiation Oncology, Room Wk-319, PO Box 2040, NL-3000, CA, Rotterdam, The Netherlands. E-mail d.robinson@erasmusmc.nl

Light fractionation using a 2-h dark interval significantly enhances the clinical response of superficial basal cell carcinoma (sBCC) to 5-aminolaevulinic acid-based photodynamic therapy (ALA-PDT) (1, 2). The increased effectiveness of this two-fold illumination scheme was first demonstrated in a series of pre-clinical studies and was optimized in the hairless mouse model (3–6). Despite these encouraging results the mechanism behind the increased effectiveness has yet to be fully elucidated. We have shown that the overall amount of protoporphyrin (PpIX) re-synthesized in the period after the first light fraction of the two-fold illumination does not correlate with the response to the treatment (6–8). Increasing the length of the dark interval from 1 to 2 h leads to a significant increase in visual skin response, despite the fact that the amount of PpIX utilized is not significantly different (7). We have also shown that light-fractionation using methyl aminolevulinate (MAL), an ester derivative of ALA, does not increase the response of normal mouse skin above that following a single light fraction (9). This is despite the fact that the application of MAL results in identical fluorescence pharmacokinetics during the two-fold illumination. A significant disadvantage of superficial fluorescence measurements is that the depth distribution of photosensitizer is not fully resolved. For thin tissues, such as the normal skin of pre-clinical models, the depth distribution of PpIX is normally neglected (6, 10–13). For thicker lesions, such as BCC, it is likely that the depth distribution is a significant confounding factor in the determination of the pharmacokinetics of PpIX. Microscopic analysis of tumour biopsies, sectioned and imaged using fluorescence microscopy, has been used previously to determine the distribution of PpIX in BCC and in other organs (14–18). Most of these studies have investigated distribution of PpIX in nodular BCC. Only one study has investigated the microscopic distribution in sBCC after topical ALA (19). In addition, the spatial distribution of PpIX re-synthesis in BCC has not been investigated. For these reasons, in the present study we investigated the spatial distribution of PpIX in sBCC undergoing light-fractionated ALA-PDT, comparing both surface and fluorescence microscopy. In addition, we investigated the presence and distribution of the proliferation marker Ki-67. Ki-67 is a protein that is detected in

 ISSN 0001-5555
doi: 10.2340/00015555-0508

the nucleus in phase G1, S, G2 and M of the cell cycle. Ki 67 is considered vital for proliferation. The number of cells with Ki-67 is used to estimate cell proliferation. In BCC an average of 20% positive cells has been reported (20–23). A uniform distribution of Ki-67-positive cells has been reported (24) suggesting an equal proliferation in neoplastic cells over the bulk of the tumour and in tumour islands. A recent study by Tilly et al. (25) found proliferate activity restricted to the periphery of tumour nests in superficial and nodular BCC. In aggressive and recurring BCC, Ki-67 expression has been shown to be higher (26). Vidal et al. (27) studied the expression of Ki-67, among others, in BCC in response to topical imiquimod treatment and found a high pre-treatment percentage of positive Ki-67 cells (39%) and no significant modification during therapy. In this study we compared the distribution of Ki-67 with the distribution of PpIX in sBCC undergoing light-fractionated ALA-PDT.

MATERIALS AND METHODS

Patients and aminolaevulinic acid application

Eight patients diagnosed with multiple sBCC were recruited to investigate the superficial and microscopic distribution of PpIX during light-fractionated ALA-PDT. The design was approved by the ethics committee of Erasmus MC, according to the Declaration of Helsinki Principles. All patients gave their informed consent. Thirty-two lesions were included in the present analysis. Where possible, four lesions were identified in each patient. The location of lesions was dependent on the patient, but sites on the back, chest, arm, face and legs were used. One lesion was randomly designated as a control lesion, to which ALA was administered but was not illuminated. The remaining three lesions underwent light-fractionated ALA-PDT. Topical ALA ointment was prepared by the hospital pharmacy using 20% ALA (FLUKA, Zwijndrecht, The Netherlands) in Instilagel® (Medeco B.V., Oud Beijerland, The Netherlands). The ointment was freshly prepared and stored in a refrigerator to be used within 7 days. Before application of ALA, crusts and scaling were removed using a disposable curette. Control and treatment lesions were covered with a margin of 1 cm and dressed with a semi-permeable dressing (Tegaderm® 3M, Leiden, The Netherlands) over aluminium foil to protect the lesion from light during the application of ALA.

Photodynamic therapy and biopsy collection

Illuminated lesions received light-fractionated ALA-PDT using a two-fold illumination scheme in which $20 + 80$ Jcm^{-2} was delivered, separated by a 2 h dark interval (1). A light fluence of 20 Jcm^{-2} was delivered 4 h after the administration of ALA, at a constant uniform fluence rate of 50 mWcm^{-2}, using a 630 nm diode laser (Carl Zeiss, Oberkochen, Germany). Immediately after the therapeutic illumination lesions were re-covered with a light protective dressing for a dark interval of 2 h. Immediately before the second light fraction, 6 h after the administration of ALA, a 5 mm punch biopsy was obtained from the centre of each lesion. Biopsy sites were stitched, and swabbed until any bleeding had stopped. The remaining lesions then received a second light fraction of 80 Jcm^{-2}. A margin of at least 5 mm around each lesion was included in each treatment field. Control lesions that did not receive the first light fraction were biopsied at the corresponding time-point, 6 h after the administration of ALA. After the punch biopsy was taken control lesions were stitched and swabbed. Control lesions did not undergo PDT in this treatment session, but were allowed to heal and subsequently treated using light-fractionated ALA-PDT.

Superficial protoporphyrin fluorescence imaging

Superficial PpIX fluorescence images were acquired to investigate the spatial kinetics of PpIX re-synthesis. Data were acquired immediately before ALA application, before and after the first illumination, and before the second illumination. Measurements were performed as described previously, using a custom applicator attached to a fluorescence-imaging camera (1). Images acquired at different time-points were registered under translation and rotation using landmarks in the skin surrounding the lesion (e.g. hair follicles). Typically, a rectangular area of 4×6 cm is imaged that includes the whole lesion and the biopsy site. Where possible the site of the biopsy was identified in each series of 3 images (acquired before and after the first light fraction and before the second light fraction). An additional image was acquired after the end of the second light fraction, used to aid the localization of the biopsy site in the series images. A circular region of interest approximately 0.5 cm in diameter is defined and the average pixel intensity was used as a measure of the fluorescence intensity from an area of tissue that coincided with the area from which the biopsy was taken. Autofluorescence was measured before each ALA application and was subtracted from the PpIX fluorescence intensity acquired before and after each illumination.

Fluorescence microscopy

Frozen skin samples were handled under subdued light conditions. Tissue-Tec® II embedding compound (Leica, Leiden, The Netherlands) was used to mount the skin sample on the sample holder of a cryostat (Leica). Cross-sections were cut and mounted singularly on glass slides (Menzel, Braunschweig, Germany). Each tumour biopsy was sectioned at three depths collecting one 20 μm section and three 5 μm sections at each depth. Tumour sections were allowed to thaw at room temperature for 30 min to one hour after sectioning before imaging. Very low intensity red light using a high-pass 695 filter was used to localize the section and focus its image. Fluorescence images were acquired using a slow-scan CCD camera (Proscan, Lagerlechfeld, Germany) mounted on a fluorescence microscope (Leitz DM RB, Leica) equipped with an N2.1 filter block. This filter combination includes a 515–560 nm band pass excitation filter and dual dichroic and long-pass detection filters (RKP580 and LP590m respectively, Leica). Light from the sample was then filtered using an additional 635 ± 5 nm interference filter (BP635, Melles Griot, Zevenaar, The Netherlands). Background and reference (KV470 filter, Schott, Tiel, The Netherlands) images were recorded for each set of fluorescence images. The fluorescence images were corrected by subtracting the corresponding background image and dividing the resulting image with the corresponding KV470 image. All images were corrected for variations in excitation light intensity. A 120 sec integration time was necessary to maximize the signal-to-noise ratio for the detection of PpIX. Longer integration times reduced the signal-to-noise ratio due to PpIX photobleaching during image acquisition.

Immunohistochemical staining

For each biopsy an additional 5 μm tumour cross section was cut immediately adjacent to the final section of the fluorescence analysis. These sections were analysed for the presence of the nuclear antigen Ki-67 proliferation marker using a method adapted from that suggested by DAKO (Heverlee, Belgium).

Fluorescence image analysis and assay scoring

For each frozen tumour biopsy, three sets of 5 and 20 μm sections cut more than 250 μm apart were used to determine the relative intensity and spatial distribution of PpIX. Sections of 20 μm were imaged using 50× magnification and 5 μm sections were imaged using the 400× magnification. Low magnification imaging was chosen so that the full thickness of the tumour and the underlying dermis could be acquired in a single image. High magnification sections provided a more detailed image of the border between tumour and normal tissue. The spatial distribution of PpIX fluorescence within the section was recorded at both high and low magnification. In addition, within each image three areas of tumour were identified and the PpIX fluorescence intensity and its standard deviation were measured in a square region of interest. The size of these regions of interest were approximately 50 × 50 and 5 × 5 μm using 50× and 400× magnification, respectively. Immunohistochemical scoring was performed without prior knowledge of the distribution of PpIX fluorescence. The overall Ki-67 score was calculated as the percentage of positively stained cells to total cells.

RESULTS

Figs 1a and 1b show the variation in the mean PpIX fluorescence intensity, measured in sections acquired from sBCC, 6 h after the administration of ALA in control lesions (C1–7) and in lesions (1, 2, 4–25) at the end of the dark interval 2 h after the delivery of the first light fraction of 20 Jcm^{-2}, 4 h after the administration of ALA. Figs 1a and 1b show the results from fluorescence analysis and 400× (5 μm sections) and 50× (20 μm sections) magnification respectively. It was not possible to identify a control lesion in one patient. Fig. 1c shows the relationship between the average PpIX fluorescence intensity using the two magnification/sectioning techniques. There is a reasonable correlation between the fluorescence intensity recorded with each technique ($R^2 = 0.86$). For both analyses of the distribution in

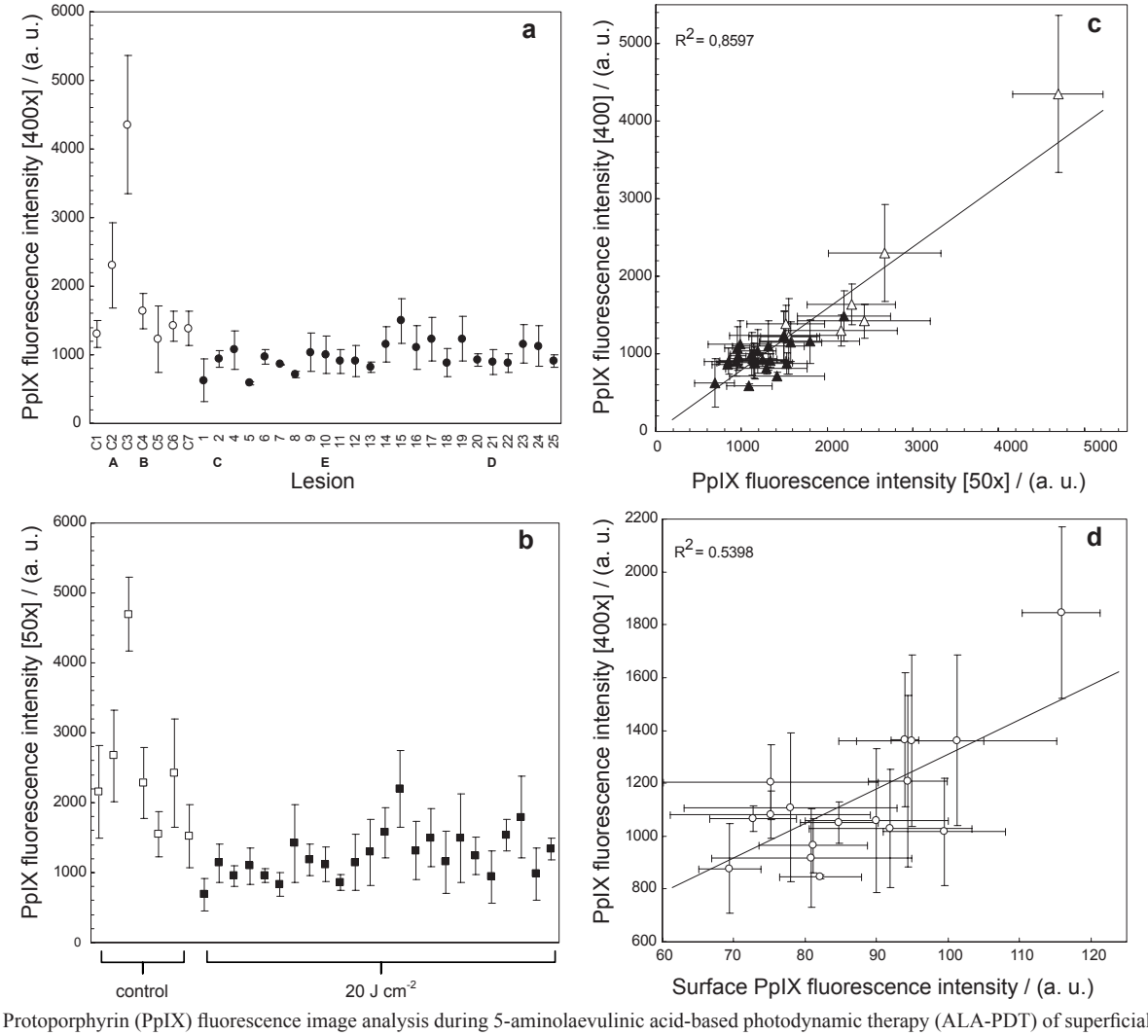

Fig. 1. Protoporphyrin (PpIX) fluorescence image analysis during 5-aminolaevulinic acid-based photodynamic therapy (ALA-PDT) of superficial basal cell carcinoma (sBCC), showing the mean microscopic fluorescence intensity measured using (a) 400× and (b) 50× magnification in control (c1–7) un-illuminated lesions 6 h after the application of 20% 5-aminolaevulinic acid (ALA) and in treated lesions (1–25) 2 h after 20 Jcm^{-2}. (c) Correlation between the microscopic fluorescence intensity measured using 50× and 400× magnification. (d) Correlation between the surface and microscopic fluorescence intensity. In all cases error bars represent standard deviations. Unfilled symbols represent unilluminated lesions. Filled symbols represent illuminated lesions. a.u.: arbitrary units. (A–E refers to the lesions of Fig. 2.).

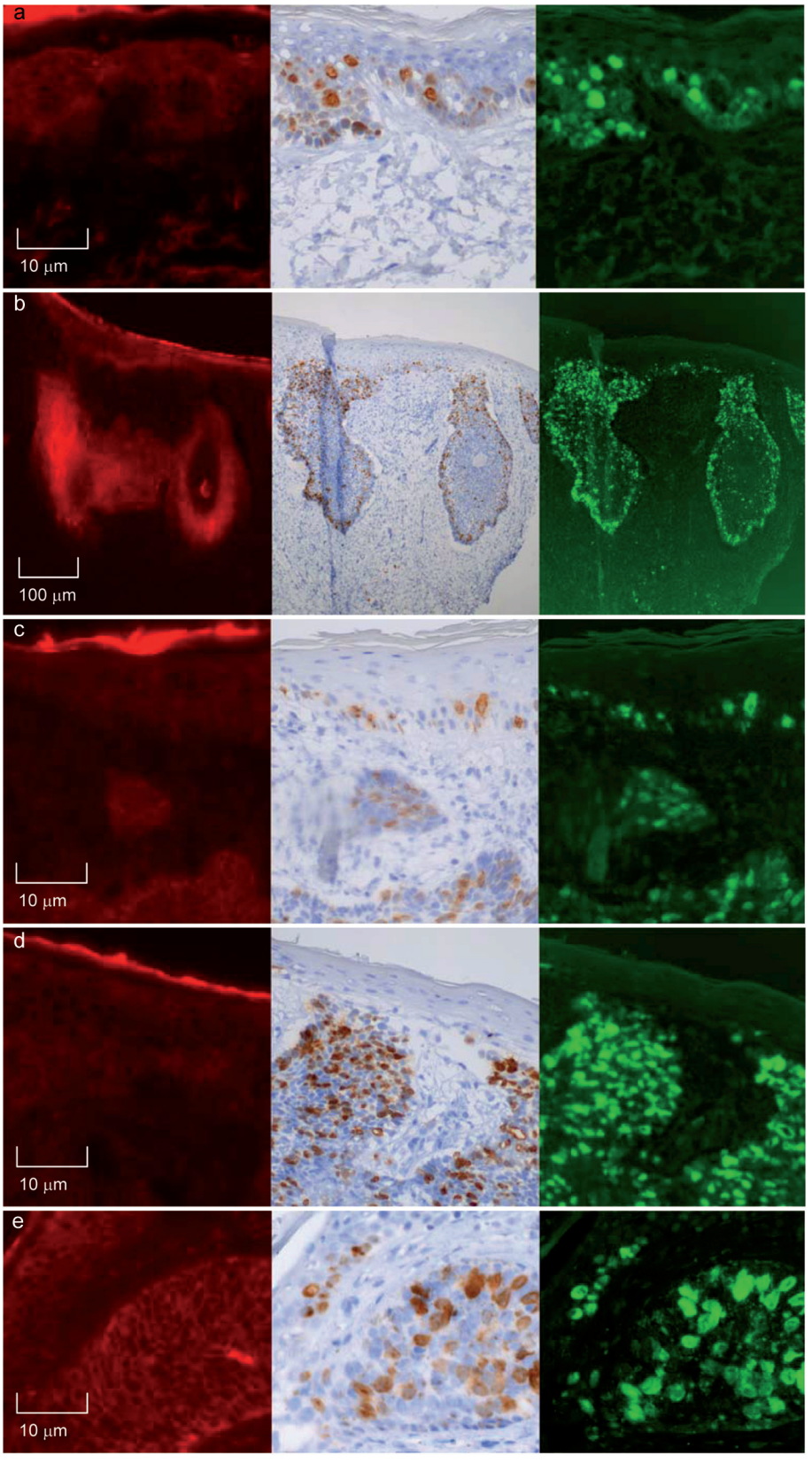

Fig. 2. Representative microscopic images of sections of superficial basal cell carcinoma (sBCC). Left image: protoporphyrin (PpIX) fluorescence distribution; middle and right images: Ki-67 staining. The middle image has been spectrally unmixed to show the distribution of Ki-67-positive cells. (a and b) Control lesions, 6 h after application of 20% 5-aminolaevulinic acid (ALA). (c–e) Sections 2 h after 20 Jcm^{-2}, and 6 h after application of 20% ALA. See detailed description in text.

PpIX fluorescence there are large variations in PpIX fluorescence intensity between individual control and illuminated lesions. The standard deviation of PpIX fluorescence calculated from weighted average of three regions of interest in three sections per biopsy are large, approximately 20–25% of the average absolute fluorescence intensity in an individual biopsy. The fluorescence intensity in control biopsies is greater than that in illuminated lesions 2 h after the end of the first light fraction. There is no significant difference between the standard deviations within and between regions of interest from individual biopsies for the control and illuminated lesions. Fig. 1d shows the relationship between the average PpIX fluorescence intensity measured using the surface collection technique and the microscopic analysis using the 400× magnification. We were able to localize the biopsy site in each of the three pre-biopsy surface images in 17 of the 25 lesions that were illuminated. There is a weak correlation between these two methods of determining the PpIX fluorescence intensity ($R^2 = 0.54$). The standard deviations for each technique are again large.

Fig. 2 show five representative tumour sections that have been analysed for PpIX fluorescence distribution (left red image) and Ki-67 positively stained cells (centre and right image). The centre Ki-67 image has undergone spectral unmixing in the right hand image, to show positively stained brown cells above the blue background stained with haematoxylin. Figs 2a and 2b show sections of control lesions that were biopsied 6 h after the administration of ALA. Fig. 2 c–e show sections of lesions that

were biopsied 2 h after 20 Jcm^{-2}, 6 h after the administration of ALA. Analysing all of the sections under high magnification, an average of 20% of tumour cells were positively stained for Ki-67 compared with the total number of tumour cells. There was no difference in the proliferation index between control or illuminated lesions. Fig. 2a shows a sBCC that extends into the upper dermis. Tumour cells in the region show significant fluorescence that extends into the upper dermis. There is a relatively uniform distribution of PpIX fluorescence in the tumour cells that includes cells that are stained Ki-67 positive and cells that are not. Fig. 2a also shows significant fluorescence deeper, which seems to be associated with collagen fibres. Fig 2b shows a 50× magnification 20 μm section of a control biopsy that shows the deeper extension of BCC into the dermis. The section illustrates peripheral palisading and retraction artefact at the boundary between tumour cells and the surrounding dermis, which are characteristic of BCC. In this section there are significant differences in the distribution of PpIX fluorescence. In the island of BCC on the left of the section there is a rather uniform distribution of fluorescence. The island of BCC on the right of the section shows a peripheral distribution of PpIX in which the centre of the island shows very little PpIX accumulation. There is no obvious general trend for a depth distribution of PpIX fluorescence in BCC. Regions of high PpIX fluorescence intensity are clearly seen in islands relatively deep in the dermis. Note that the very centre of this island shows a fluorescence artefact that is probably due to fluorescence from the glass beneath the section that is exposed due to the hole in the section clearly seen in the central Ki-67 image. In this section the distribution of Ki-67-positive cells closely follows the distribution of PpIX. The interior of the island on the right shows very little or no Ki-67-positive cells, while the island on the left of the sections shows a more uniform distribution of Ki-67-positive cells. Fig. 2c shows a section of an illuminated lesion 2 h after PDT, showing the basal layer of the epidermis and an island of BCC between the epidermis and a deeper lying region of tumour cells. In the superficial layers of the section there is a relatively uniform distribution of PpIX fluorescence that includes cells that are stained Ki-67-positive and cells that are not. In the tumour island and in the lower region of the image PpIX fluorescence closely corresponds to Ki-67-positive cells. Figs 2d and 2e show in more detail the border between tumour cells and cells of the dermis. Again, there is a moderate correlation between PpIX fluorescence intensity and Ki-67-positive cells in regions of tumour cells outside the epidermis where positive and negative Ki-67 cells accumulate PpIX. Again, we did not observe a systematic trend for differences in the overall distribution of PpIX between control and illuminated lesions. However, PpIX fluorescence in biopsies that were illuminated and imaged at 400× magnification were somewhat more diffuse than control images. This suggests that there may have been a slightly different sub-cellular distribution of PpIX 2 h after PDT compared with the distribution of PpIX 6 h after the administration of ALA. It is important to note that an intense fluorescence signal is observed in all sections that include the most superficial layers of the skin with either intact stratum corneum or tumour crusts.

Fig. 3 shows the variation in mean surface PpIX fluorescence during, before and after the first light fraction and at the end of the dark interval immediately before the second light fraction. Again, it was only possible to recover data for the whole sequence of images in 17 of the 25 lesions that received PDT. The PpIX fluorescence before the first light fraction varied considerably. The mean normalized fluorescence after the illumination is 48% of that before the first light fraction and rises to 63% during the 2 h dark interval. This compares with a mean surface fluorescence intensity in control, non-illuminated lesions, that is 119% of the average immediately prior to the first light fraction, 4 h after the administration of ALA. During PpIX fluorescence, photobleaching varied widely despite fixed illumination parameters. The average extent of photobleaching, of 47% during the first light fraction, is similar to that found in our pre-clinical studies (3, 5–7).

DISCUSSION

The purpose of this study was to investigate the distribution of PpIX in sBCC, during light-fractionated

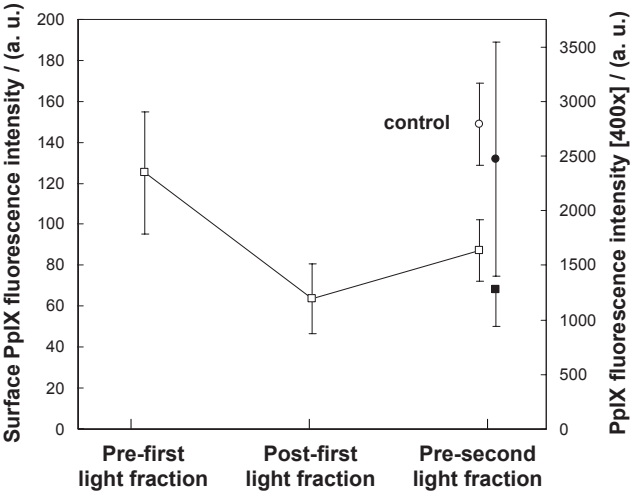

Fig. 3. Kinetics of surface protoporphyrin (PpIX) fluorescence intensity in superficial basal cell carcinoma (sBCC) during 5-aminolaevulinic acid-based photodynamic therapy (ALA-PDT) with a two-fold illumination scheme (open squares) delivering 20 Jcm^{-2} and the re-synthesis during the 2 h dark interval between light fractions and the PpIX fluorescence in un-illuminated control lesions (open circle – left axis). The corresponding mean microscopic PpIX fluorescence intensity (closed symbols – right axis) is shown for comparison. In all cases error bars represent standard deviations.

ALA-PDT, using fluorescence microscopy. We found wide variations in the average intensity of PpIX fluorescence in biopsies of control lesions and in biopsies of lesions 2 h after illumination with 20 Jcm^{-2}. We also found wide variations in fluorescence intensity within individual sections of biopsies. The large variability in fluorescence intensity measured in adjacent tumour sections is likely to be a consequence of the difficulty of making sections of reproducible thickness. Also, since tissue sectioning is known to disrupt cell and organelle membranes, it is possible that PpIX bound at lipophilic sites within the tissue localizes in different environment(s) that induce unpredictable variations in fluorescence quantum yield of PpIX. This is a particular problem for thin (5 μm) sections. Given these large standard deviations on average fluorescence intensities, we found a reasonable correlation between the two different methods of performing fluorescence microscopy (Fig. 1c). The biopsy average PpIX fluorescence intensity determined using 20 μm sections and 50× magnification was similar to that determined using 5 μm micron sections and 400× magnification. This is an encouraging result that adds some weight to the use of semi-quantitative fluorescence microscopy as a method of determining PpIX intensity. Large variations in microscopic PpIX content after ALA administration have been observed previously in BCC. Martin et al. (19) attributed these variations to differences in ALA penetration through intact stratum corneum and ALA transport within individual tumours. The transport of ALA in large nodular tumours is clearly an important parameter that influences the synthesis of PpIX at depth. However, in the present study we have shown for sBCC, where ALA penetration and transport are unlikely to be limiting factors, there remain regions of tumour that accumulate and re-synthesize relatively small amounts of PpIX. It is also clear that regions of low PpIX fluorescence accumulation are not located at the base of superficial tumours and high PpIX fluorescence is often observed at the periphery of tumour islands at the base of the tumour, as seen in Fig. 2b. Clearly there are other more important mechanism(s) that influence the synthesis of PpIX in sBCC when high concentrations of ALA are present. As long ago as 1997, Peng et al. (28) were able to review the literature and conclude that PpIX is preferentially synthesized in tumours and in rapidly dividing cells. Our present data supports these general conclusions. More rapidly dividing tumour cells at the base of sBCC, that are Ki-67 positive synthesize relativity more PpIX. The underlying mechanism behind the differential synthesis is complex, but it is thought to be a consequence of the relative activity of enzymes within the biosynthetic pathway of heme, in particular porphobilinogen deaminase and ferrochelatase (29). In the present study we have shown that, even in sBCC, where the local availability of ALA is not a limiting factor, significant numbers of tumour cells synthesize relatively low amounts of PpIX. Reduced PpIX synthesis, at depth, where the concentration of ALA is limited has been suggested as an important factor in the reduced response of nodular BCC following ALA-PDT. Our results suggest that the ability of cells to synthesize PpIX is also an important consideration. In this case modification of heme biosynthesis, particularly in cells that do not synthesize sufficient PpIX, seems an attractive option (30).

The large spatial variations in distribution of PpIX fluorescence, in particular the variations associated with depth, illustrate the challenge for fluorescence detection of sBCC, which is frequently advocated as a method of optical diagnosis (31–34). Recently Stenquist et al. (35) published data describing the use of fluorescence imaging to demarcate the boundaries of BCC during Mohs' micrographic surgery. A mapping precision of ± 3 mm was estimated. The authors used uncorrected *in vivo* fluorescence imagining.

As noted above, we observe a fluorescent layer in the most superficial layers of the stratum corneum, the origin of this fluorescence is unknown and may be an artefact of the sectioning process.

The fact that we have found similar spatial distributions of PpIX, 2 h after the first light fraction of 20 Jcm^{-2}, compared with un-illuminated control biopsies, confirms our recent pre-clinical findings that there is no significant influence of PDT on the ability of cells or tissue to re-synthesize PpIX and that there is little evidence for a systemic component of PpIX re-synthesis (36). The average amount of PpIX that is re-synthesized during the 2 h dark interval after the first light fraction measured using fluorescence microscopy and superficial imaging are consistent with those that we have observed previously (1, 2). The present study does, however, illustrate the inherent weakness of spatial averaging of tissues in which there is large variation in the spatial (re-)synthesis of PpIX.

We are continuing to investigate the mechanism behind the response of tissues to light-fractionated ALA-PDT. With regard to the underlying mechanism, it is important to note that all of the illuminated lesions investigated in the present study showed complete response to light-fractionated ALA-PDT 24 months after therapy. This is in spite of the significant variations in microscopic PpIX fluorescence intensity measured immediately before the second light fraction. While the mechanism behind this increased response is not yet completely clear, we have shown that the average kinetics of superficial PpIX fluorescence may be misleading (9). Our data for mouse skin indicate that the microscopic distribution of PpIX after the application of ALA is an important aspect in the response of tissues to light-fractionated ALA-PDT.

In conclusion, we have measured the spatial microscopic distribution of PpIX in sBCC and shown the

wide variations between tumour cells and within and between tumour biopsies. We have the confirmed that the relative re-synthesis of PpIX after PDT is consistent with that recently found in pre-clinical models (6). We have shown that highly proliferating normal and tumour cells synthesize relatively more PpIX and that this corresponds with Ki-67 staining. We have shown that, even in sBCC, there are significant regions of tumour cells that do not synthesize PpIX even when there is sufficient ALA availability. The clinical relevance of these variations in PpIX fluorescence for light-fractionated ALA-PDT requires further investigation.

REFERENCES

1. de Haas ERM, Kruijt B, Sterenborg HJCM, Neumann HAM, Robinson DJ. Fractionated illumination significantly improves the response of superficial basal cell carcinoma to aminolevulinic-acid photodynamic therapy. J Invest Dermatol 2006; 126: 2679–2686.
2. Star W, van 't Veen AJ, Robinson DJ, Munte K, de Haas ERM, Sterenborg HJCM. 5-aminolaevulinic acid mediated photodynamic therapy of superficial basal cell carcinoma using two light fractions with a two hour interval. Acta Derm Venereol 2006; 86: 412–417.
3. van der Veen N, van Leengoed HLLM, Star WM. In vivo fluorescence kinetics and photodynamic therapy using 5-aminolaevulinic acid-induced porphyrin: increased damage after multiple irradiations. Br J Cancer 1994; 70: 867–872.
4. van der Veen N, Hebeda KM, de Bruijn HS, Star WM. Photodynamic effectiveness and vasoconstriction in hairless mouse skin after topical 5-aminolevulinic acid and single or two-fold illumination. Photochem Photobiol 1999; 70: 921–929.
5. de Bruijn HS, van der Veen N, Robinson DJ, Star WM. Improvement of systemic 5-aminolevulinic acid photodynamic therapy in vivo using light fractionation with a 75-minute interval. Cancer Res 1999; 59: 901–904.
6. Robinson DJ, de Bruijn HS, Star WM, Sterenborg HJCM. Dose and timing of the first light fraction in two-fold illumination schemes for topical ALA-mediated photodynamic therapy of hairless mouse skin. Photochem Photobiol 2003; 77: 319–323.
7. de Bruijn HS, van der Ploeg-van den Heuvel A, Sterenborg HJCM, Robinson DJ. Fractionated illumination after topical application of 5-aminolevulinic acid on normal skin of hairless mice; the influence of the dark interval. J Photochem Photobiol B Biol 2006; 85: 184–190.
8. de Bruijn HS, Sluiter W, van der Ploeg-van den Heuvel A, Sterenborg HJCM, Robinson DJ. Evidence for a bystander role of neutrophils in systemic ALA-PDT using a two-fold illumination scheme. Photodermatol Photoimmunol Photomed 2006; 22: 238–246.
9. de Bruijn HS, de Haas ERM, Hebeda KM, van der Ploeg-van den Heuvel A, Sterenborg HJCM, Neumann HAM, et al. Light fractionation does not enhance the efficacy of methyl 5-aminolevulinate mediated photodynamic therapy in normal mouse skin. Photochem Photobiol Sci 2007; 12: 1325–1331.
10. Thissen MRTM, Robinson DJ, de Blois AW, de Bruijn HS, Dutrieux RP, Star WM, et al. PpIX fluorescence kinetics and increased skin damage after intracutaneous injection of 5-aminolevulinic acid and repeated illumination. J Invest Dermatol 2002; 118: 239–245
11. Moan J, Ma LW, Iani V, Juzeniene A. Influence of light exposure on the kinetics of protoporphyrin IX formation in normal skin of hairless mice after topical application of 5-aminolevulinic acid methyl ester. J Invest Dermatol 2005; 125: 1039–1044.
12. Juzenas P, Juzeniene A, Kaalhus O, Iani V, Moan J. Noninvasive fluorescence excitation spectroscopy during application of 5-aminolevulinic acid in vivo. Photochem Photobiol Sci 2002; 1: 745–748.
13. Amelink A, van den Heuvel A, de Wolf WJ, Robinson DJ, Sterenborg HJCM. Monitoring PDT by means of superficial reflectance spectroscopy J Photochem Photobiol B Biol 2005; 79: 243–251.
14. Tope WD, Ross EV, Kollias N, Martin A, Gillies R, Anderson RR. Protoporphyrin IX fluorescence induced in basal cell carcinoma by oral delta-aminolevulinic acid. Photochem Photobiol 1998; 67: 249–255.
15. Heyerdahl H, Wang I, Liu DL, Berg R, Andersson-Engels S, Peng Q, et al. Pharmacokinetic studies on 5-aminolevulinic acid-induced protoporphyrin IX accumulation in tumours and normal tissues. Cancer Lett 1997; 112: 225–231.
16. Peng Q, Warloe T, Moan J, Heyerdahl H, Steen HB, Nesland JM, et al. Distribution of 5-aminolevulinic acid-induced porphyrins in noduloulcerative basal cell carcinoma. Photochem Photobiol 1995; 62: 906–913.
17. Leunig A, Mehlmann M, Betz C, Stepp H, Arbogast S, Grevers G, et al. Fluorescence staining of oral cancer using a topical application of 5-aminolevulinic acid: fluorescence microscopic studies. J Photochem Photobiol B 2001; 60: 44–49.
18. Fehr MK, Wyss P, Tromberg BJ, Krasieva T, DiSaia PJ, Lin F, et al. Selective photosensitizer localization in the human endometrium after intrauterine application of 5-aminolevulinic acid. Am J Obstet Gynecol 1996; 175: 1253–1259.
19. Martin A, Tope WD, Grevelink JM, Starr JC, Fewkes JL, Flotte TJ, et al. Lack of selectivity of protoporphyrin IX fluorescence for basal cell carcinoma after topical application of 5-aminolevulinic acid: implications for photodynamic treatment. Arch Dermatol Res 1995; 287: 665–674.
20. Baum HP, Meurer I, Unteregger G. Ki67 antigen expression and growth pattern of basal cell carcinomas. Arch Dermatol Res 1993; 285: 291–295.
21. Horlock HM, Wilson GD, Daley FM, Richman PI, Sanders R. Cellular proliferation characteristics of basal cell carcinoma: relationship to clinical subtype and histopathology. Eur J Surg Oncol 1997; 23: 247–252.
22. Chang CH, Tsai RK, Chen GS, Yu HS, Chai CY. Expression of bcl-2, p53 and ki-67 in arsenic skin cancers. J Cutan Pathol 1998; 25: 457–462.
23. Tilli CMLJ, Stavast-Kooy AJW, Ramaekers FCS, Neumann HAM. Bax expression and growth behavior of basal cell carcinomas. J Cutan Pathol 2002; 29: 79–87.
24. Abdelsayed RA, Guijarro-Rojas M, Ibrahim NA Sangueza OP. Immunohistochemical evaluation of basal cell carcinomas and trichoepithelioma using Bcl-2, Ki67 PCNA and P53. J Cutan Pathol 2000; 27: 169.
25. Tilli CMLJ, Van Steensel MAMA, Krekels GAM, Neumann HAM, Ramaekers FCS. Molecular aetiology and pathogenesis of basal cell carcinoma. Br J Dermatol 2005; 152: 1108–1124.
26. Healy E, Angus B, Lawrence CM, Rees JL. Prognostic value of Ki67 antigen expression in basal cell carcinomas. Br J Dermatol 1995; 133: 737–741.
27. Vidal D, Matias-Guiu X, Alomar A. Efficacy of imiquimod for the expression of Bcl-2, Ki67, p53 and basal cell carcinoma apoptosis. Br J Dermatol 2004; 151: 656–662.
28. Peng Q, Warloe T, Berg K, Moan J, Kongshaug M,

Giercksky KE, et al. 5-Aminolevulinic acid-based photodynamic therapy. Clinical research and future challenges. Cancer 1997; 79: 2282–2308.
29. Hinnen P, de Rooij FW, van Velthuysen ML, Edixhoven A, van Hillegersberg R, Tilanus HW, et al. Biochemical basis of 5-aminolaevulinic acid-induced protoporphyrin IX accumulation: a study in patients with (pre)malignant lesions of the oesophagus. Br J Cancer 1998; 78: 679–682.
30. Curnow A, McIlroy BW, Postle-Hacon MJ, Porter JB, MacRobert AJ, Bown SG. Enhancement of 5-aminolaevulinic acid-induced photodynamic therapy in normal rat colon using hydroxypyridinone iron-chelating agents. Br J Cancer 1998; 78: 1278–1282.
31. Vereecken P, Da Costa CM, Steels E, De Lathouwer O, Heenen M, De Mey A. Fluorescence diagnosis of face-located basal cell carcinomas: a new dermatological procedure which may help the surgeon. Acta Chir Belg 2007; 107: 205–207.
32. Won Y, Hong SH, Yu HY, Kwon YH, Yun SJ, Lee SC, et al. Photodetection of basal cell carcinoma using methyl 5-aminolaevulinate-induced protoporphyrin IX based on fluorescence image analysis. Clin Exp Dermatol 2007; 32: 423–429.
33. Ericson MB, Sandberg C, Gudmundson F, Rosen A, Larkö O, Wennberg AM. Fluorescence contrast and threshold limit: implications for photodynamic diagnosis of basal cell carcinoma. J Photochem Photobiol B 2003; 69: 121–127.
34. Andersson-Engels S, Canti G, Cubeddu R, Eker C, af Klinteberg C, Pifferi A, et al. Preliminary evaluation of two fluorescence imaging methods for the detection and the delineation of basal cell carcinomas of the skin. Lasers Surg Med 2000; 26: 76–82.
35. Stenquist B, Ericson MB, Strandeberg C, Mölne L, Rosen A, Larkö O, et al. Bispectral fluorescence imaging of aggressive basal cell carcinoma combined with histopathological mapping: a preliminary study indicating a possible adjunct to Mohs micrographic surgery. Br J Dermatol 2006; 154: 305–309.
36. de Bruijn HS, Kruijt B, van der Ploeg-van den Heuvel A, Sterenborg HJCM, Robinson DJ. Increase in protoporphyrin IX after 5-aminolevulinic acid based photodynamic therapy is due to local re-synthesis. Photochem Photobiol Sci 2007; 8: 857–864.